Fabrication of Biocompatible and UV Absorbing Active Ingredients

in Sunscreen by Electron Irradiation

Sangyoon Lee[a], Hyung San Lim[a], Na Eun Lee[a], Sung Oh Cho*
[a,*]Department of Nuclear and Quantum Engineering, KAIST, Daejeon 34141, Republic of Korea
*socho@kaist.ac.kr

1. Introduction

UV radiation is a sort of electromagnetic wave and it can be subdivided into three bands, UV-A (315-400 nm), UV-B (280-315 nm), and UV-C (100-280 nm) recommended by ISO standard 21348 [1]. UV-C is completely absorbed by the atmosphere and the others partially reach the human skin [2]. Short-term exposure to UV-B induces cholecalciferol (vitamin D_3) synthesis. On the other hand, long-term exposure can cause detrimental effects such as skin aging, sunburn, or even skin cancers through direct DNA damage [3, 4]. Due to stratospheric ozone depletion, ultraviolet index has been increased and skin cancer incidence has accordingly been increased [5]. Currently, 3 million non-melanoma skin cancers, and 132,000 melanoma skin cancers occur globally each year according to WHO estimates. Therefore, sunscreens are globally used as precautions to reduce adverse health effects of UV exposure but ironically, they have safety issues. Commercial active ingredients in organic sunscreen such as avobenzone (AVO), octocrylene (OC) are known to cause endocrine disruption and inorganic ingredients such as zinc oxide, and titanium oxide generate reactive oxygen species (ROS) through photo-oxidation [10 - 13]. The maximum concentrations of all the ingredients are restricted by regulatory agencies and specialists recommend customers to use sunscreen with low UV filter concentration rather than other chemical-rich products. In order to avoid ironic situations using toxic or phototoxic substances as a precaution, it is necessary to develop non-toxic UV filtering ingredients.

In previous research, various efforts to develop non-toxic UV absorbers have been made in order to substitute the conventional toxic sunscreens. Encapsulation of the UV absorbers into biocompatible materials showed enhanced safety, but the mechanical stabilities of the capsules or uniformities are not guaranteed [14, 15]. In this study, we propose novel active ingredients developed by irradiation of an electron beam onto PMMA and PS polymers. Both polymers are biocompatible in pristine states and they are not suspected as biodegradable, bio-accumulative, nor environmental toxins. In addition, they are currently being used in cosmetics as viscosity increasing agents or film formers. UV absorption characteristics that are not present in pristine states are created to X-ray, electron beam, or ion beam irradiated PMMA and PS [16 – 18]. In this study, in order to modify the polymers effectively, the polymers were irradiated by 50 keV electron beam that has high linear energy transfer values. Plus, the particle size was determined considering size effect on light scattering from a viewpoint of UV shielding. For being used as active ingredients in sunscreen, various electron irradiation conditions were altered and tested to create UV absorptive properties on PMMA and PS nanoparticles with their initial biocompatible traits maintained.

2. Experimental

Sample Preparation

The polymer PMMA (SOKEN Chemical & Engineering Co., Ltd) and PS (Magsphere, Inc., Pasadena, CA) used in this study was obtained in a powder form with a diameter of 150 nm. When the particle size is comparable to the wavelength of the light, rather than much smaller or much larger, there is an important size dependent scattering. In the light interaction, not only absorption but also backscattering can be a part of shielding. According to Mie theory, when the particle size is similar or slightly larger than incident light, the portion of the forward scattering is greater than when it is not. The schematic representation of Mie scattering is shown in figure 1. Considering the sizing effect, PMMA and PS nanoparticles with a diameter of 150 nm were investigated to better shield the harmful UV light which wavelength of interest is 280 to 400 nm.

Fig. 1. Schematic illustration of Rayleigh scattering and Mie scattering

Since PMMA and PS both are insulating materials, charge can be build up during electron irradiation. The charge buildup makes nanoparticles physically unstable due to the repulsive force generated. In order to conduct irradiation experiments on insulating nanoparticles, a solution casting method was used. First, 200 mg of nanoparticles was dispersed in 2ml of de-ionized water at room temperature. Then, the aqueous suspension is sonicated to have a homogeneously dispersed suspension. The suspension was drop-casted into a metallic substrate and heated on a hot plate at 40℃. The dried suspension turn to a consolidated thin powder film.

ESTAR Monte Carlo simulation estimates 50keV electron has a continuous slowing down approximation (CSDA) range of 37.6 μm in PMMA. In order to minimize charge buildup, the powder film is prepared with a thickness of less than 15 μm.

Electron Beam Irradiation

Irradiation experiments were conducted in a vacuum chamber under a pressure of 10^{-5} Torr using a thermionic electron gun equipped with a tantalum cathode (Fig. 2). The irradiation stage was cooled down to avoid thermal damage during irradiation using a chiller. The temperature was set at -5°C. 50 keV electron beam was used to irradiate the powder film and beam current density was 0.4 μA/cm^2. The fluence was controlled by irradiation time.

Fig. 2. Electron beam generator used in this work.

Characterization

UV-Vis spectrometer (Perkin Elmer, Lambda 1050) was used to record optical absorption spectra in the diffuse reflectance mode and it covers the spectral range from 200 to 800nm. Chemical structures of the pristine and irradiated powder films were analyzed by FTIR spectrometer (Thermo Fisher Scientific Instrument, Nicolet IS50 FTIR) and Raman spectrometer (Bruker, RFS 100/S) in the range of 400-4000 cm^{-1}. In addition, ^{1}H NMR analysis was performed at 22°C in this study (Agilent 400MHz 54mm NMR DD2) in the range of 0 to 10 ppm. Solvent of 99.96% deuterated CDCl3 was used for the NMR sample with 0.03% of Tetramethylsilane (TMS) as a referencing material.

In order to estimate the phototoxicity of electron irradiated PMMA and PS, the 3T3 Neutral Red Uptake phototoxicity test (3T3 NRU PT) was carried out in accordance with the guideline from OECD TG 432. Chlorpromazine (CPZ) is used as positive control in this study. The phototoxicity is analyzed by comparing with phototoxic reactions between chemicals and UV exposed chemicals. To determine the phototoxicity, photo irritation factor (PIF) and mean photo effect (MPE) are calculated by software, Phototox 2.0 from the concentration response curves obtained in the presence and absence of UV.

In order to evaluate the UV absorbing performance of electron irradiated PMMA and PS nanoparticles in sunscreen products, sun protection factor (SPF) and protection of UVA (PA) of test sunscreens containing the powders were calculated according to the international standard, determination of sunscreen UVA photo-protection in vitro (ISO 24443). Following the guideline, 32.5 milligrams of emulsion were applied over the entire surface (25 cm^2) on a HD6 plate using a finger cot. Test sunscreens for the determination of two factors are prepared by the combination of 25% of irradiated particles, 52.5% of deionized water, and 22.5% of ethanol. Deionized water and ethanol here were used as bases of test sunscreens with no UV-A and UV-B absorbing properties. UV-Vis spectroscopy in total transmission mode over the wavelength region of UV were analyzed using an integrating sphere. The calculations were carried out according to the following equations:

$$SPF_{in\ vitro} = \frac{\int_{\lambda=290}^{\lambda=400} E(\lambda) \times I(\lambda) \times d\lambda}{\int_{\lambda=290}^{\lambda=400} E(\lambda) \times I(\lambda) \times 10^{-A_0(\lambda) \times C} \times d\lambda} \quad (1)$$

$$UVPAF_0 = \frac{\int_{\lambda=320}^{\lambda=400} P(\lambda) \times I(\lambda) \times d\lambda}{\int_{\lambda=320}^{\lambda=400} P(\lambda) \times I(\lambda) \times 10^{-A_0(\lambda) \times C} \times d\lambda} \quad (2)$$

where $E(\lambda)$ is the erythema action spectrum, $I(\lambda)$ is the spectral irradiance received from the UV source (SSR for SPF testing), $A_0(\lambda)$ is the mean monochromatic absorbance of the test product layer before UV exposure, $P(\lambda)$ is the persistent pigment darkening (PPD) action spectrum, and $d\lambda$ is the wavelength step (1nm). These two factors fundamentally indicate the inverse of mean UV transmission weighted by $I(\lambda)$ and $P(\lambda)$ or $E(\lambda)$.

3. Results

The UV-Visible absorption spectra of pristine and irradiated PMMA powder films are shown in figure 3. The spectra show that the absorption in the spectral range of ultraviolet wavelength (200-400nm) is significantly increased by electron irradiation. In addition, the absorption edge redshifts to longer wavelength with the increase in electron fluence. To understand this phenomenon, FTIR and Raman spectroscopies were carried out (Fig. 4 and 5). It is observed that the pendant groups of pristine PMMA are dissociated by electron irradiation. Interestingly, there is only one peak generated by electron irradiation at the wavenumber of 1640 cm^{-1}. The indicated peak is not present in pristine state and it is more clearly seen in Raman spectra. Dissociation of the pendant groups makes the bond radical and the spare electrons can be combined, forming sp^2 bonds in the backbone. New π electrons that are not present in pristine PMMA have lower optical bandgap than pristine PMMA. Therefore, the newly generated π bond in the irradiated PMMA begins to absorb ultraviolet rays that could not be absorbed by pristine PMMA which only have sigma electrons or single bonds. As the fluence of electron beam increases, π electrons generated in the surrounding units can be conjugated. According to Pauli's exclusion principle, the energy level of sp^2 electrons split. This reduces the optical bandgap that is the difference

between highest occupied molecular orbital (HOMO) and lowest unoccupied molecular orbital (LUMO) in the irradiated PMMA. The conjugation process elucidates the redshift phenomenon of absorption spectra in UV-Vis spectroscopy.
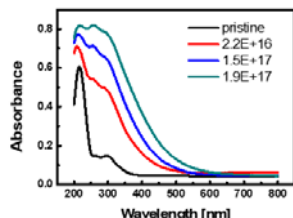

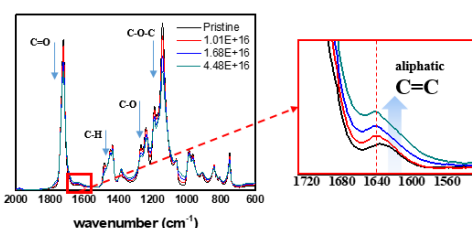Fig. 3. UV-Vis spectra of pristine and irradiated PMMA

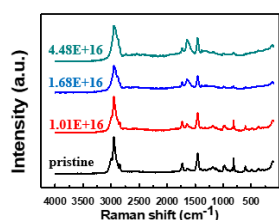Fig. 4. FTIR spectra of pristine and irradiated PMMA

Fig. 5. Raman spectra of pristine and irradiated PMMA

The results of the UV-Vis study of pristine and irradiated PS powder films shows very similar changes with that of PMMA and shown in figure 6. The absorption in the spectral range of ultraviolet wavelength is increased and the spectra redshifts to longer wavelength with the increase in electron fluence. In order to elucidate this phenomenon, FTIR, Raman, and ^{1}H NMR spectroscopies were carried out. FTIR and Raman spectra is shown in figure 7. It is observed that the pendant groups of pristine PS are dissociated by electron irradiation. The results of FTIR and Raman were distinct from that of PMMA. No new peak was detected in irradiated PS. Since polystyrene possess only hydrogen and carbons, the changes by electron irradiation were not easily detected by FTIR and Raman spectroscopies. The result of ^{1}H NMR reveals the structural changes in the electron irradiated PS. In the downfield region in figure 8, there are new peaks indicating conjugated aromatic hydrocarbons which are not present in pristine PS. The resonance peaks are assigned to 1, 2: biphenyl, terphenyl, phenyl naphthalene. Dissociation of benzene rings in the pristine PS makes the phenyl radical and it can adhere to other radical, forming conjugated aromatic hydrocarbons. The π electrons associated in conjugated bonds have lower optical bandgap than pristine.

Therefore, the newly generated π electrons in the irradiated PS begins to absorb ultraviolet rays that could not be absorbed by pristine PS. As the fluence of electron beam increases, conjugation length increases. Due to the conjugation, the optical bandgap is lowered and absorption spectra in UV-Vis redshifts.
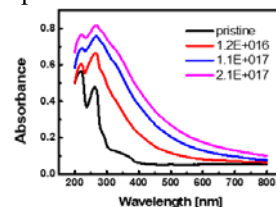

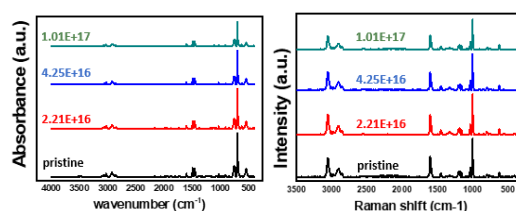
Fig. 6. UV-Vis spectra of pristine and irradiated PS

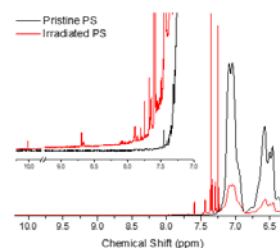Fig. 7. FTIR and Raman spectra of pristine and irradiated PS

Fig. 8. ^{1}H NMR spectra of pristine and irradiated PS

Figure 9 shows the cell viabilities with respect to the eight different concentrations of irradiated PMMA. Chlorpromazine is used as a positive control. The OECD guideline provides the classification criteria that are shown in Table 1. The result of 3T3 NRU phototoxicity test is seen in Table 0. According to the guideline, pristine and electron irradiated PMMA with the fluence of 4.48E+16 e/cm^2 both are classified as non-phototoxic materials.
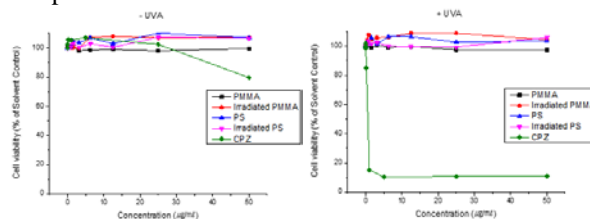

Fig. 9. Cell viabilities of pristine and irradiated polymers

Materials	PIF	MPE	Classification
Pristine PMMA	1.3	-0.02	No phototoxicity
EB irradiated PMMA	1.0	-0.02	No phototoxicity
Pristine PS	1.0	-0.01	No phototoxicity
EB irradiated PS	1.0	-0.05	No phototoxicity
CPZ (positive control)	48.3	0.32	Phototoxicity

Table. 1. PIF and MPE values of pristine and irradiated polymers

Figure 10 shows the sun protection factor and protection of UV-A of test sunscreen containing 25% of electron irradiated PMMA and PS. The electron fluence varies from 0 to 2.1E+17e/cm^2. Both PMMA and PS of irradiated more than 1.1E+16e/cm^2 have SPF values of higher than 5 which stand comparison with other commercial ingredients. Table 0 shows the SPF and PA values of sunscreens containing irradiated particles and commercial ingredients. The concentration of commercial ingredients are decided as the highest US FDA approved concentrations. The PA values from 2 to 4, 4 to 8, and higher than 8 are classified as PA+, PA++, and PA+++ respectively.
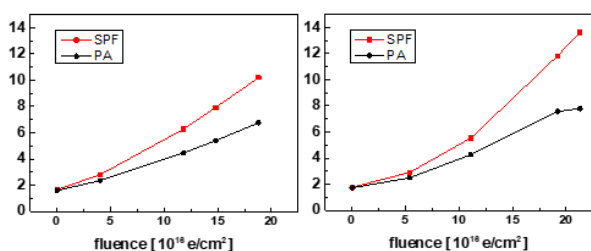

Fig. 10. Sun protection factor of test sunscreen containing pristine and variously irradiated polymers

		SPF $_{in\ vitro}$	PA$_0$
organic	Avobenzone (3%)	2.7	3.1
	Oxybenzone (6%)	1.5	1.5
	Octocrylene (10%)	7.2	3.3
	Octinoxate (7.5%)	8.1	1.9
	Octisalate (5%)	1.9	1.1
	Homosalate (15%)	2.3	1.2
inorganic	TiO2 (25%)	3.5	3.3
	ZnO (25%)	3.2	3.3

Table. 2. SPF and PA values of test sunscreen containing commercial ingredients

4. Conclusion

In this study, non-toxic active ingredients in sunscreen were fabricated by electron irradiation on PMMA and PS nanoparticles. Aliphatic carbon double bonds and conjugated aromatic hydrocarbons in PMMA and PS respectively emerges as the UV absorptive traits when irradiated by 50 keV electron beam. The conjugation length increases at higher electron fluence, elucidating the redshift phenomenon of UV-Vis absorption spectra in both PMMA and PS. Plus, the irradiated PMMA was classified as non-phototoxic material according to the OECD guideline. Furthermore, UV absorbing performance of irradiated polymeric powders in sunscreen was measured by sun screening factors, in vitro SPF and PA in accordance with ISO 24443. Irradiated PMMA and PS nanoparticles not only reflect the UV due to the size effect, but also absorb UV-A and UV-B. Test sunscreens containing these nanoparticles at fluence of higher than 1.1E+17e/cm^2 show promising sun screening performances comparing to commercial sunscreens.

REFERENCES

[1] "ISO 21348 Definitions of Solar Irradiance Spectral Categories" (2013)
[2] Haigh, Joanna D. "The sun and the Earth's climate", Living Reviews in Solar Physics, 4, (2007), 2
[3] William J. Olds, Alex R. McKinley, Michael R. Moore, Michael G. Kimlin, "In vitro model of vitamin D3 (Cholecalciferol) synthesis by UV radiation: Dose–response relationships", Journal of Photochemistry and Photobiology B: Biology 93 (2008) 88–93
[4] Svobodová AR, Galandáková A, Sianská J, et al., "DNA damage after acute exposure of mice skin to physiological doses of UVB and UVA light". Arch Dermatol Res. 304 (5): (2012) 407–412
[5] R. L. McKenzie,*a P. J. Aucamp,b A. F. Bais,c L. O. Bjorn, ¨ d,e M. Ilyasf and S. Madronichg, "Ozone depletion and climate change: impacts on UV radiation", Photochemical & Photobiological Sciences 10 (2011) 182-198
[10] Chunxia Xu, Adele Green, Alfio Parisi, and Peter G. Parsons, "Photosensitization of the Sunscreen Octyl p-Dimethylaminobenzoate by UVA in Human Melanocytes but not in Keratinocytes". Photochemistry and Photobiology. 73 (6): 600–604 (2001)
[11] John Knowland, Edward A. McKenzie, Peter J. McHugh, Nigel A. Cridland, "Sunlight-induced mutagenicity of a common sunscreen ingredient". FEBS Letters. 324 (3): 309–313 (1993)
[12] S. T. Butt, Terje Christensen, "Toxicity and Phototoxicity of Chemical Sun Filters", Radiation Protection Dosimetry, 91(1) (2000)
[13] Yu Hang Leung, Xiaoying Xu, Angel P. Y. Ma, et al., "Toxicity of ZnO and TiO2 to Escherichia coli cells", Scientific Reports 6, 35243 (2016)
[14] Pey-Shiuan Wu, Lan-Ni Huang, Yi-Cing Guo, Chih-Chien Lin, "Effects of the novel poly(methyl methacrylate) (PMMA)-encapsulated organic ultraviolet (UV) filters on the UV absorbance and in vitro sun protection factor (SPF)", Journal of Photochemistry and Photobiology B: Biology, 131 (2014) 24-30
[15] Ioana Lacatusu, Nicoleta Badea, Alina Murariu, Aurelia Meghea, "The encapsulation effect of UV molecular absorbers into biocompatible lipid nanoparticles", Nanoscale Research Letters (2011) 6:73
[16] Ismayil, V. Ravindrachary, R.F. Bhajantri, et al., "Optical and microstructural studies on electron irradiated PMMA: A positron annihilation study", Polymer Degradation and Stability 95 (2010) 1083-1091
[17] Courtney P. Ennis and Ralf I. Kaiser, "Mechanistical studies on the electron-induced degradation of polymethylmethacrylate and Kapton", Physical Chemistry Chemical Physics, Issue 45 (2010)
[18] R. D. Mathad , H. G. Harish Kumar , B. Sannakki, et al., "High energy electron irradiation effects on polystyrene films", Radiation Effects & Defects in Solids, Vol. 164, No. 10, (2009) 656–664